NMR Solution Structure and Membrane Interaction of the N-Terminal Sequence (1−30) of the Bovine Prion Protein[†]

Henrik Biverståhl, August Andersson, Astrid Gräslund, and Lena Mäler*

Department of Biochemistry and Biophysics, Arrhenius Laboratory, Stockholm University, 10691 Stockholm, Sweden

Received July 14, 2004; Revised Manuscript Received September 14, 2004

ABSTRACT: The structure and membrane interaction of the N-terminal sequence (1−30) of the bovine prion protein (bPrPp) has been investigated by NMR spectroscopy in phospholipid membrane mimetic systems. CD spectroscopy revealed that the peptide adopts a largely α-helical structure in zwitterionic bicelles as well as in DHPC micelles but has a less degree of α-helix structure in partly charged bicelles. The solution structure of bPrPp was determined in DHPC micelles, and an α-helix was found between residues Ser8 and Ile21. The residues within the helical region show slow amide hydrogen exchange. Translational diffusion measurements in zwitterionic $q = 0.5$ bicelles show that the peptide does not induce aggregation of the bicelles. Increased quadrupolar splittings were observed in the outer part of the ^{2}H spectrum of DMPC in $q = 3.5$ bicelles, indicating that the peptide induces a certain degree of order in the bilayer. The amide hydrogen exchange and the ^{2}H NMR results are consistent with a slight positive hydrophobic mismatch and that bPrPp forms a stable helix that inserts in a transmembrane location in the bilayer. The structure of bPrPp and its position in the membrane may be relevant for the understanding of how the N-terminal (1−30) part of the bovine PrP functions as a cell-penetrating peptide. These findings may lead to a better understanding of how the prion protein accumulates at the membrane surface and also how the conversion into the scrapie form is carried out.

Prion proteins are glycoproteins associated with neurodegenerative diseases called spongiform transmissible encephalopathies (TSE) (*1*) occurring in a variety of mammals. The most known among these diseases are bovine spongiform encephalopathy (BSE) in cattle and Creutzfeldt−Jacob disease (CJD) in humans. The diseases are characterized by the accumulation of a pathological form of the host-encoded prion protein (PrP)[1] in the infected mammal's brain (*2*−*4*). Prion diseases can have infectious, sporadic, or familiar origin (*5*−*7*). The disease is associated with the conversion of the nontoxic cellular form of the prion protein (PrP^C) into the abnormally folded aggregated isoform (PrP^{Sc}). These two forms have very different physical properties. PrP^C is monomeric and easily digested by proteinase K, while PrP^{Sc} forms highly insoluble aggregates and shows a high resistance to proteolytic digestion (*8*). The cellular trafficking, turnover, and membrane interactions of PrP have recently attracted considerable attention, since these processes are believed to be of crucial importance for the infection as well as the structure conversion associated with disease (*9*−*12*). The mature form of PrP is a glycoprotein, anchored at the plasma membrane by a C-terminal glycosyl phosphatidylinositol anchor, exposing the protein to the extracellular side (*13*−*15*). The effects of membrane interactions on the structure of PrPs have been the subject of several studies (*11*, *12*, *16*−*18*).

NMR studies of the solution structure of the mature form of bovine PrP (residues 23−230) in aqueous solution show a flexibly disordered N-terminal segment (residues 23−124) and a globular C-terminal domain extending from residue 125 (*19*). The basic sequence (residues 23−28) resembles a nuclear localization sequence (NLS) and appears to have an important role for internalization of a prion protein via endocytosis in neurons (*10*). The N-terminal sequence, ranging from residue 23 to around residue 100, has been shown to be responsible for internalization of the entire prion protein (*10*, *20*, *21*). By mutation of one of the Lys residues in the N-terminal NLS-like sequence (residues 23−28) it was shown that the internalization by endocytosis was completely abolished.

The N-terminal segment of newly synthesized PrP contains a signal sequence (residues 1−22). The N-terminal part (residues 1−28) of mouse PrP, including the signal sequence, functions as a cell penetrating peptide (CPP), able to facilitate the transport of large hydrophilic cargoes through a cell membrane (*22*, *23*). It has further been demonstrated that the peptide could adopt a wide range of secondary structures, ranging from α-helical in neutral vesicles to mostly β-sheet structure in negatively charged vesicles and that the β-structure was associated with aggregated peptides (*23*). However, no solution structure has been determined, and it is not clear

[†] This work was supported by grants from the Swedish Research Council (to A.G. and L.M.) and by grants from the European Commission (to A.G., contracts HPRN-CT-2001-00242 and QLK3-CT-2002-01989).

* Corresponding author. E-mail: lena.maler@dbb.su.se. Phone: +46 8 162448. Fax: +46 8 155597.

[1] Abbreviations: bPrP, bovine prion protein; bPrPp, N-terminal (1−30) sequence of bPrP; NMR, nuclear magnetic resonance; TOCSY, total correlation spectroscopy; NOESY, nuclear Overhauser enhancement spectroscopy; DHPC, 1,2-dihexanoyl-*sn*-glycero-3-phosphatidylcholine; DMPC, 1,2-dimyristoyl-*sn*-glycero-3-phosphatidylcholine; DMPG, 1,2-dimyristoyl-*sn*-glycero-3-phospho-1-glycerol; rmsd, root mean square deviation.

10.1021/bi0485070 CCC: $27.50
Published on Web 11/02/2004

in which way the peptide interacts with the membrane.

During biogenesis at the ER membrane, PrP adopts various topological forms. It is not yet clear how these forms are generated, but the N-terminal may, as suggested, have two separate functions, both targeting and topogenesis (*24*−*27*). One of these forms, ^{Ctm}PrP, which has been suggested to play an important role for the pathogenesis for the prion diseases, has been found to contain an uncleaved N-terminal signal peptide (*28*). However, recent results show that scrapie infection does not affect the quantitative levels of either ^{Ctm}PrP or untranslocated (presumably cytosolic) PrP, both containing an uncleaved signal peptide, thus suggesting that these two forms are unlikely neurotoxic intermediates in prion diseases (*29*), although other studies show that retrotranslocated cytosolic PrP without signal peptide is neurotoxic (*30*, *31*). It is possible that such improperly trafficked forms of PrP could directly mediate both the infectious and the structure conversion processes involving the prion proteins.

The mechanism of action of CPPs is a subject of intense investigation, both in model systems and in cells. Lately, it has been argued that more than one mechanism must exist and that a combination of them is responsible for the internalization process. In addition to biological processes, such as endocytosis, an energy-independent mechanism has been observed, which seems to be dependent on the presence of basic amino acid residues and on membrane potential (*32*).

The present study concerns the N-terminal domain (residues 1−30) of the bovine PrP (bPrPp) and its membrane interactions. This domain corresponds to the previously studied mouse PrP (1−28), and like the mouse peptide, bPrPp is a CPP (to be published). We argue that this N-terminal peptide, possibly important for the pathogenesis of the prion diseases, may confer new membrane interaction properties to PrP: facilitated membrane translocation by CPP activity may influence infectivity, and membrane-induced structure conversions may affect the stability of the structure of the remaining protein and affect membrane integrity. It is therefore of interest to clarify the molecular details of the membrane interactions of the peptide. The peptide has the sequence MVKSKIGSWILVLFVAMWSDVGLCKKRPKP and includes the NLS-like sequence (residues K25−P30) and the signal sequence upstream of the NLS sequence. We have determined the NMR solution structure of bPrPp in a membrane-mimetic medium with DHPC micelles, and we have investigated the interactions between the peptide and the phospholipids in zwitterionic bicelles by a variety of NMR methods.

MATERIALS AND METHODS

Sample Preparation. The N-terminal sequence (1−30) of bovine PrP was obtained as a custom synthesis from Neosystem Laboratories (Strasbourg, France;, immunograde purity) and was used without further purification. Both deuterated and undeuterated phospholipids, dihexanoyl-*sn*-glycero-3-phosphatidylcholine-d_{22} (DHPC-d_{22}), dimyristoyl-*sn*-glycero-3-phosphatidylcholine-d_{54} (DMPC-d_{54}), dihexanoyl-*sn*-glycero-3-phosphatidylcholine (DHPC), and dimyristoyl-*sn*-glycero-3-phosphatidylcholine (DMPC), were purchased from Avanti Polar Lipids Inc. (Alabaster, AL).

Micelle-containing samples were prepared by dissolving 1 mM bPrPp powder in 100 mM DHPC-d_{22}. The sample was vortexed and centrifuged and transferred to an NMR tube. ^2H_2O (10%) was added for field/frequency lock stabilization. Between measurements the sample was rapidly frozen in liquid nitrogen and stored in the freezer. In the ^2H_2O exchange experiments the sample was lyophilized in the NMR tube, and 600 μL of ^2H_2O was added. The sample was inserted immediately after in the NMR spectrometer. Bicelle samples were produced by mixing 1 M DHPC with a slurry of DMPC or DMPG/DMPC in H_2O to obtain a sample with a lipid concentration of 17% (w/v) and q = 0.5. In ^{2}H NMR, the q-value was 3.5, but otherwise the bicelle samples were produced in the same way. Samples containing bPrPp were produced by dissolving the peptide in the bicelle solution. The samples were vortexed and centrifuged until a clear solution was obtained. For the diffusion measurements the peptide concentration was 1 mM. Quadrupolar splittings were measured for the bicelles and for bicelles in the presence of 3 and 6 mM bPrPp.

Spectroscopy. CD spectra were recorded for bPrPp in aqueous solution, phosphate buffer solution, DHPC micelles, DMPC/DHPC bicelles (q = 0.5), and DMPC/DMPG/DHPC bicelles (q = 0.5, DMPG/DMPC = 0.25). The CD measurements were made on a Jasco J-720 CD spectropolarimeter with a 0.01 mm quartz cuvette. Wavelengths from 190 to 250 nm were measured, with a 0.5 nm step resolution and 100 nm/min speed. The response time was 4 s, with 50 mdeg sensitivity and a 5 nm bandwidth. A PTC-343 controller regulated the temperature. Spectra were collected and averaged over 12 scans. To interpret the CD spectra the JASCO program J-700 standard analysis for Windows was used. The α-helical content was estimated from the amplitude at 222 nm (*33*), assuming that only α-helix and random coil conformations contribute to the CD spectrum. The peptide concentration in the samples was determined by light absorption on a CARY 4 spectrophotometer, using cuvettes with 1 cm light path. All spectra were baseline corrected. A molar absorptivity of 11200 M^{-1} cm^{-1} at 280 nm wavelength for two tryptophans was applied. All CD measurements were recorded at 37 °C.

The two-dimensional ^{1}H NMR experiments were performed on a Varian Inova spectrometer equipped with a triple-resonance probe head operating at 800 MHz ^{1}H frequency. The spectral width was 10000 Hz in both dimensions, and the spectra were collected with 2048 data points in the ω_2 dimension and 512 in the ω_1 dimension. Before Fourier transformation the data were zero filled to 4096 data points in ω_2 and 2048 in ω_1. Two-dimensional TOCSY spectra (*34*) were recorded with mixing times of 60 and 30 ms, and the two-dimensional NOESY spectra (*35*) were recorded with mixing times of τ_m = 100 ms and τ_m = 150 ms. Water suppression was achieved with low-power presaturation or with the WATERGATE sequence (*36*). Chemical shifts were referenced to the internal chemical shifts of the lipids. All spectra were collected at a temperature of 37 °C. Spectra were processed with the program Felix (version 2000.1) on a Silicon Graphics O_2 workstation. Amide ^{1}H exchange measurements in DHPC micelles were performed by recording consecutive NOESY spectra, separated by 6 h, during a total period of 48 h. The sample for the exchange measurements was produced by lyophilizing a sample prepared in H_2O and redissolving it in ^2H_2O.

The diffusion experiments were recorded using a Varian Inova spectrometer, operating at 600 MHz ^{1}H frequency, using a triple-resonance probe head. Translational diffusion experiments were carried out using the modified Stejskal−Tanner spin−echo experiments with a gradient prepulse (*37*−*39*). The PFG was used with a maximum power of ∼60 G/cm. The diffusion measurements for the bicelle and micelle samples were carried out using fixed time intervals and 30 linearly incremented power levels, from 1/30 to maximum power. The T_1 delay was set to 0.15 s in measurements on the bicelle sample and to 0.07 s in the DHPC sample. For the H_2O sample, 30 linearly incremented power levels, ranging from 1/30 to 1/2 maximum power, were used and the T_1 delay was set to 0.01 s. The accuracy in the diffusion measurements was improved by correcting for nonlinear gradients according to Damberg et al. (*40*). All diffusion experiments were recorded at 37 °C. Diffusion coefficients can be related to the size and shape of the molecule or aggregate. The value of the translational diffusion coefficient, *D*, is given by the Stokes−Einstein relation:

$$D = \frac{kT}{6\pi\eta R_H F_p} \quad (1)$$

where R_H is the radius of hydration, k is the Boltzmann constant, η is the viscosity, and F_p is the Perrin shape factor. For an oblate (disk-shaped) object, F_p is given by (*41*)

$$F_p = \frac{\sqrt{(a/b)^2 - 1}}{(a/b)^{2/3} \arctan\sqrt{(a/b)^2 - 1}} \quad (2)$$

in which a is the long axis of the disk and b is the short axis. This ratio has been related to the q-value of a bicelle (*42*, *43*), resulting in

$$a/b = \frac{1}{2}[2 + kq(\pi + \sqrt{\pi^2 + 8k/q})] \quad (3)$$

where k is the ratio of the headgroup areas of DHPC as compared to DMPC. For bicelles with $q = 0.5$ this results in $F_p = 1.22$.

The ^{2}H NMR experiments were carried out at 61.4 MHz ^{2}H frequency (400 MHz ^{1}H frequency) using a Bruker Avance spectrometer. The spectra were acquired with a double-resonance probe head using the standard quadrupolar echo sequence $\pi/2-\tau_1-\pi/2-\tau_2-$acq (*44*), where $\tau_1 = 50$ μs and $\tau_2 = 40$ μs and with a $\pi/2$ pulse width of 14.75 μs. The pulse width was measured at 15 °C, where the isotropic phase of the bicelles prevails. Typically 2048−4096 transients were accumulated. The data were collected at 25, 30, 37, and 40 °C. The temperature was calibrated using a thermocouple, which was inserted in a regular NMR tube containing H_2O. The magnitude of the measured quadrupolar splittings (Δ) can be related to the segmental order parameter of the C−^{2}H bond and can be described by an order parameter, S_{CD}. For a bicelle, aligned with its normal perpendicular to the static magnetic field, this relation is given by

$$\Delta = \frac{3}{2}\left(\frac{e^2qQ}{h}\right)S_{CD}\left(\frac{1}{2}\right) \quad (4)$$

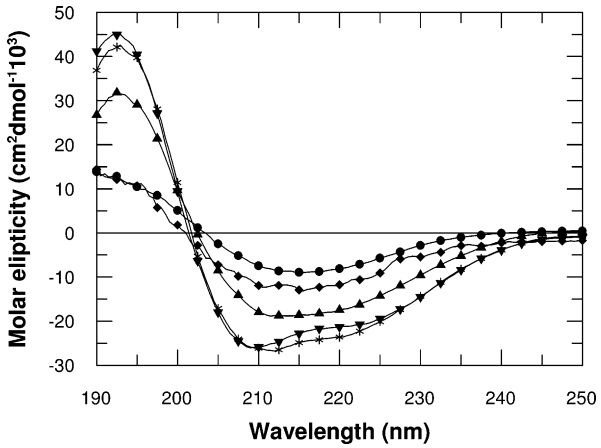

FIGURE 1: CD spectra for bovine bPrPp(1−30) in different solvents. The temperature was 37 °C, and the concentration of peptide was 1 mM. The spectra were recorded in water (◆), phosphate buffer (●), 100 mM DHPC micelles (▼), DMPC/DHPC bicelles (*), and $q = 0.5$ DMPG/DMPC/DHPC bicelles (DMPG/DMPC = 0.25) (▲).

in which e^2qQ/h is the quadrupolar coupling constant (∼168 kHz for an alkyl C−^{2}H bond) (*45*).

Structure Calculation. Distance constraints were generated from quantifying NOESY cross-peak intensities as described earlier (*46*). Cross-peaks were categorized into three different groups, with upper distance limits of 3.5, 4.5, and 6.0 Å, respectively, based on their intensities. The upper distance limits were normalized against known distances. A total of 241 distance constraints (87 intramolecular, 81 sequential, and 73 medium range) were obtained from the NOESY spectra with $\tau_m = 100$ ms. Structures were calculated with the program DYANA (*47*), version 1.5, using torsion angle dynamics. Standard annealing algorithms were used, and a total of 60 structures were calculated. A final ensemble of 22 structures was selected, based on their target function and constraint violations, to represent the solution structure. The quality of the structure was checked with the program PROCHECK_NMR (*48*). Visual analyses of the solution structures were made with INSIGHT (version 2000; Accelrys). The coordinates of the final structure together with the input constraints have been deposited with the PDB under accession code 1SKH.

RESULTS

Structure of bPrPp in DHPC Micelles and DMPC/DHPC Bicelles. CD measurements were performed to establish the effects of different solvents on the secondary structure of bPrPp. Figure 1 shows CD spectra for bPrPp in water, bPrPp in phosphate buffer, DHPC micelles, DMPC/DHPC bicelles, and DMPG/DMPC/DHPC bicelles. These CD results show that the structure of the peptide becomes α-helical in both DHPC and DMPC/DHPC bicelles. The amount of induced helical structure was estimated from the mean molar ellipticity at 222 nm, and it was seen that bPrPp adopts a similar amount of helical structure in both membrane mimetics (62% vs 66%). Interestingly, the same amount of helical structure is not seen in partly charged bicelles, where instead a fairly high degree of β-sheet structure is observed, consistent with findings in unilamellar vesicles (*49*). This is also observed in both buffer solution and in pure H_2O, where the peptide is mainly in random coil and in β-sheet conformation. Although bicelle solution is considered to be a more accurate

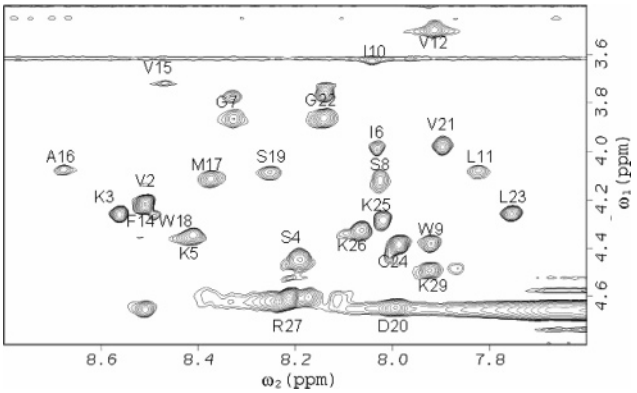

FIGURE 2: Part of the 800 MHz TOCSY spectrum recorded for 1 mM bPrPp in 100 mM DHPC at 37 °C. The H^N-H^α region is displayed with the assigned residues indicated.

membrane mimetic than that provided by DHPC micelles, we used DHPC micelles in the NMR experiments. Bicelles were first tested; however, the NMR signals were too broad to obtain reasonable spectra; in fact, most resonances were absent in the spectra. CD measurements were also carried out to see that the NMR sample did not aggregate over time, and it was seen that the sample was stable for at least a period of 12 days in 37 °C.

The 2D NMR spectra in DHPC micelles were of sufficient quality to obtain high-resolution structural data. Resonance assignments for the protons were obtained from the TOCSY spectra recorded with $\tau_{mix} = 30$ ms and $\tau_{mix} = 60$ ms (Figure 2), and sequential assignments were obtained from H^N-H^N and H^N-H^α connectivities in the NOESY spectrum obtained with $\tau_{mix} = 100$ ms. The secondary $^1H^\alpha$ chemical shifts were calculated according to Wishart and Sykes (*50*), and chemical shifts characteristic of a helical structure were found for residues Gly7 through Asp20 (Figure 3a). This indicates a helical content of about 50%, in good agreement with the CD results in DHPC. NOE data support the finding of a helical structure, by characteristic medium-range NOE cross-peaks ranging from Lys5 to Leu23 (Figure 3b), although the NOEs were classified as weak at the termini. NOE cross-peak connectivities could readily be found for the N-terminal part of the peptide, while very few NOE cross-peaks were observed for the C-terminus (the NLS-like part).

In all, 241 distance constraints were obtained by quantifying cross-peaks in the NOESY spectrum obtained with the shorter mixing time (100 ms). A solution structure of bPrPp was calculated on the basis of the distance constraints, and the ensemble of 22 structures is shown in Figure 4. Structural statistics for the ensemble of 22 models are presented in Table 1. The structure is in good agreement with the data as the distance violations are small (the average maximum violation is 0.10 Å) and shows good Ramachandran statistics with most residues in the allowed regions. On the basis of analyses of backbone torsion angles and hydrogen-bonding patterns, an α-helical structure was assigned for residues Ser8 through Val21. A putative hydrogen bond from Asp20 HN to Met17 O is only present in 11 of 22 structures, but the regular α-helical hydrogen bond between Val21 HN and Met17 O is present in 19 structures, indicating a somewhat irregular helical structure at the C-terminus of the helix. Furthermore, a kink is seen at Ala16, which shows characteristics of a 3_{10} helix. No long-range constraints were found

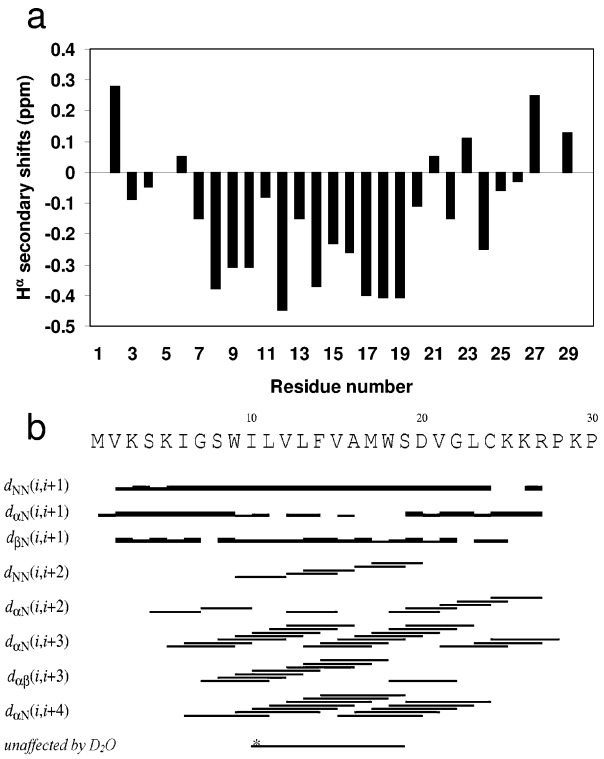

FIGURE 3: Structural data for bPrPp. (a) Secondary H^α chemical shifts. (b) Summary of NOE connectivities originating from intensities in the 2D NOESY spectra. The residues for which H^N-H^α cross-peak intensities are unaffected in the D_2O exchange experiments are also displayed. The cross-peak for Ile10 disappears after 32 h, indicated by an asterisk (*).

in the NOESY spectrum, indicating that the structure consists of a single helix, flanked by two unstructured termini. The helical part of the peptide is well determined, with a rmsd in backbone atoms of 0.26 Å (Table 1).

H^N Exchange in bPrPp. The ^2H_2O exchange experiment was performed to observe which residues that readily exchange their H^N protons. Seven NOESY spectra with $\tau_{mix} = 100$ ms were recorded with a 6 h interval to investigate the time dependence of the ^2H_2O exchange. After 6 h all cross-peaks in the H^N-H^α fingerprint region, except those belonging to residues Ile10 through Ser19, had disappeared completely. After 32 h, the cross-peak belonging to Ile10 had also disappeared. The remaining cross-peaks were still present after 48 h. These results indicate that the peptide has a stable helical core or that the helix is deeply buried within the interior of the micelle protecting it from the solvent.

Position of bPrPp in Magnetically Aligned Bicelles. To investigate the effect of the peptide on the lipids and how the peptide is positioned relative to the bilayer, ^2H NMR spectra were recorded of magnetically aligned bicelles with DMPC-d_{54} with and without the bPrPp. The size of the quadrupolar splitting is proportional to the order parameter for the $C-^2H$ bond vector of the lipid chain. The DMPC phospholipid fatty acid chain contains 14 carbons, of which 13 are carrying ^2H atoms, and all 13 ^2H sites of the lipid chain in the bicelle sample could be identified in the ^2H spectrum, although somewhat overlapped (Figure 5). The spectrum exhibits quadrupolar splittings ranging from 2320 to 19232 kHz, where the largest splitting was assigned to position 6 in the acyl chain and the smallest to the end methyl

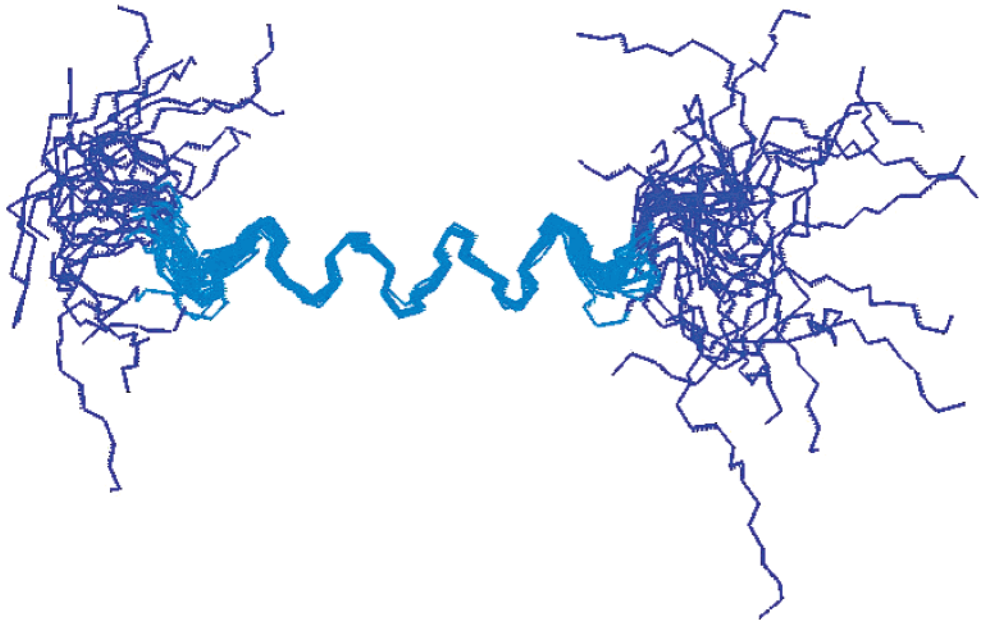

FIGURE 4: Solution structure of bPrPp in DHPC micelles as represented by an ensemble of 22 structures. The structures were superimposed on backbone atoms in residues Ser8−Val21. The helical region, Ser8−Val21, is indicated by a light blue color, while the termini are in dark blue.

Table 1: Structural Statistics for the Ensemble of 22 bPrPp Structures in DHPC Micelles Calculated with DYANA

no. of constraints	241
DYANA target function (Å^2)	$(3.0 \pm 2.2) \times 10^{-2}$
maximum distance violation (Å)	0.10 ± 0.03
backbone atom rmsd (Å)	
all residues	2.87
residues 8−21	0.26
Ramachandran plot regions (%)	
most favored	70.5
allowed region	18.2
generously allowed	8.9
disallowed	2.4

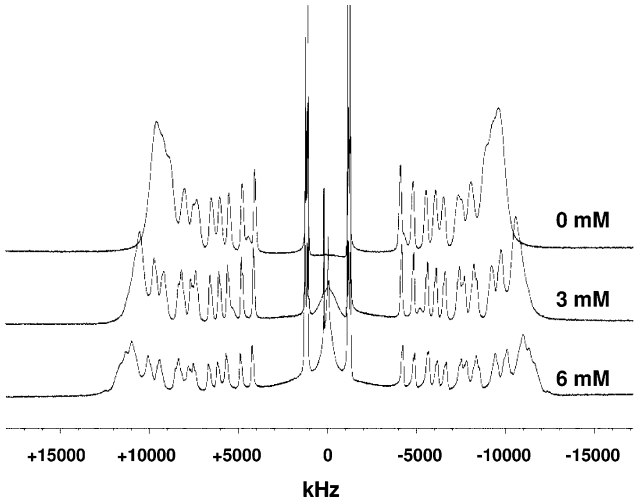

FIGURE 5: ^{2}H NMR spectra for magnetically aligned $q = 3.5$ DMPC/DHPC bicelles recorded at 40 °C. bPrPp was added to the bicelle sample to obtain the indicated peptide concentration. The total lipid concentration was 240 mM.

groups, according to Urbina et al. (*51*). Spectra with different amounts of bPrPp, 3 and 6 mM concentration, added to the bicelle sample containing 186 mM DMPC were subsequently recorded (Figure 5). It was generally observed that the peptide had the effect of increasing the quadrupolar splittings,

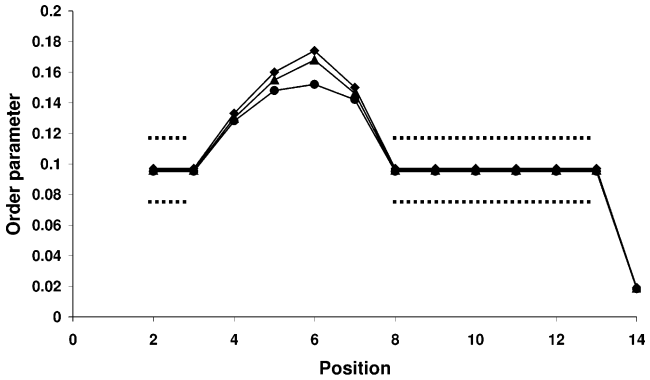

FIGURE 6: Order parameters for the DMPC-d_{54} fatty acid chain in magnetically aligned $q = 3.5$ DMPC/DHPC bicelles with and without bPrPp. Order parameters were calculated for DMPC without bPrPp (●), with 3 mM bPrPp (▲), and with 6 mM bPrPp (◆). The order parameters for positions 2, 3, and 8−13 are reported as the mean value for these sites, due to difficulties in assigning the positions separately. The dotted line represents the standard deviation for positions 2, 3, and 8−13.

hence increasing the order parameter (Figure 5). The most pronounced effects were seen for the outer methylene splittings, corresponding to positions 5 and 6 in the acyl chain, while less effect was observed for the methyl group splittings or the methylene positions at the termini of the acyl chain. Generally, the quadrupolar splitting is related to an order parameter, S_{CD}, according to eq 4. This order parameter is used to describe the increase, or decrease, in the order of the membrane. Figure 6 shows the order parameter profile for the chain carbons in DMPC with different amount of bPrPp added. The largest order parameters are observed for positions 4 through 7 in the aliphatic chain. The increase in quadrupolar splitting for the outer peaks (from 19232 to 21984 kHz) corresponds to an increase in the S_{CD} order parameter of 0.022, which is a small but still significant increase. Similar results have been observed for helical transmembrane model peptides, which were

Table 2: Translational Diffusion Constants Measured for bPrPp and Phospholipids in $q = 0.5$ Neutral Bicelle Solution and in DHPC Micelle Solution

	$D_{obs}(\times 10^{-11}$ m^2/s)			
sample	bPrPp[a]	DMPC[b]	DHPC	HDO
bPrPp in neutral bicelles		2.6	5.2	
neutral bicelles		2.9	5.5	
bPrPp in DHPC micelles	8.8		12.0	246
DHPC micelles			12.7	246

[a] Based on measurements for the aromatic signals. [b] Based on measurements for the methyl signal of the aliphatic chain of the phospholipid.

interpreted in terms of positive hydrophobic mismatch (*52*−*54*).

Diffusion. Since hardly any signals were observed in the spectrum of the peptide in $q = 0.5$ phospholipid bicelles, diffusion data were recorded to investigate potential aggregation. The diffusion data are collected in Table 2. Using $F_p = 1.22$ calculated from eq 3, together with $T = 310$ K, and assuming $\eta = 10^{-3}$ kg/ms, one finds that from the diffusion coefficients for the pure bicelle $R_H = 6.41$ nm is obtained, and with the added peptide $R_H = 7.15$ nm is obtained. From the value of R_H it is possible to relate to the dimensions of the bicelle according to the relation of the volume of a sphere and an oblate ellipsoid:

$$R_H = \sqrt{a^2 b} \tag{5}$$

Thus the dimensions of the bicelle without the peptide, given by the long axis (a) and the short axis (b), are found to be $a = 105$ Å and $b = 23.8$ Å. The figures are reasonable considering the geometrical aspects of a bicelle, the effects of a hydration layer, and the possibility for DHPC to exist as a monomer in solution (*55*). When the peptide is added, the dimensions change to $a = 117$ Å and $b = 26.6$ Å. Since this is not a radical change in the size of the bicelles, we conclude that the lack of peptide signals in the bicelle sample is not due to aggregation of several bicelles to produce large phospholipid aggregates. We do not observe any significant loss of lipid signal intensity upon addition of peptide, further indicating that bicelle aggregation does not occur. The difference in estimated bicelle dimension may, however, be a result of several peptides aggregating on the bicelle surface. One can from the diffusion data estimate the molecular weight of the bicelle aggregate, and using an average lipid density of 1000 kg/m^3, the concentration of bicelle aggregates becomes around 0.2 mM. Thus, the peptide:bicelle molar ratio is 5:1, and most likely several peptides reside within one bicelle. The diffusion data for the peptide in DHPC micelles show that the peptide on the average has a slower diffusion than DHPC, consistent with a certain amount of DHPC being free in solution (*55*, *56*) while the peptide is fully bound to the micelles.

DISCUSSION

The N-terminal part of PrP has been suggested to act as a cell-penetrating peptide (*23*). It has also been speculated that this property may in fact be related to the internalization of the entire protein. In this study we have investigated the structure of the bPrPp peptide in DHPC micelles and its effect on DMPC phospholipids in bicelles. The central part of the bPrPp peptide, ranging from residue Ser8 to Ile21, is shown to adopt an α-helical structure in DHPC micelles. There are certain indications that the helical character persists at both termini, although the NMR data reveal a disordered structure at both termini. A similar amount of helical structure is also observed in zwitterionic bicelles, as evidenced by CD measurements, and it is therefore reasonable to believe that the structure is similar in the two membrane-mimetic media. This is in agreement with CD results for the mouse PrP(1−28) peptide, where a helical conformation dominated in small unilamellar POPC vesicles (*23*). The helix does not seem to possess the amphipathic property, characteristic for cell-penetrating peptides in general, and the central residues in the helical structure are more hydrophobic than what is seen in, for instance, the typical cell-penetrating peptide penetratin. Bovine PrPp is prone to aggregation, and the structure induction in the presence of a membrane may well be correlated with the peptide aggregation propensity. The NLS sequence at the C-terminus is seen to be unstructured, which is hardly surprising considering the amino acid sequence of this part of the peptide. This part of the peptide is from amide proton exchange seen to be on the outside of the micelle. This may be important, since it has been shown that this sequence is largely responsible for the internalization of the prion protein into cells (*24*, *57*). Thus it would seem that structure is not an important factor governing the translocation of the peptide but, rather, the details in peptide−membrane interactions.

The structure in DHPC seems remarkably stable over time, as only amide proton exchange is observed for the very terminal residues of the helix (residues Ser8−Ile10 and Asp20−Val21). This is, on the other hand, likely to be the result of the peptide residing within the interior of the micelle, protecting the amide protons from the external solvent, since the amide exchange rate for residues in a free peptide in solution is much faster (*58*, *59*). To investigate more specifically the interaction between the peptide and a membrane surface, ^{2}H NMR spectra of d_{54}-labeled DMPC in bicelles were analyzed. The results show clearly that the peptide affects the membrane order. The effects are not dramatic, which indicates that the peptide does not disrupt the bicelle structure in any severe way leading to a phase change. Considering the relatively low concentration of the peptide, the changes in quadrupolar splittings are, however, significant for positions 5 through 7 in the lipid acyl chain. Transmembrane helices typically have the effect of increasing the quadrupolar splittings, and thus the order parameter of the acyl chains, if a mismatch in the helix length and the hydrophobic bilayer thickness exists (*52*, *54*). In the present investigation, the helix core contains 14−16 amino acid residues, which amounts to a helix length of around 23 Å. The hydrophobic core of the DMPC bilayer is reported to be 23 Å (*60*). Depending on the peptide sequence, including the nature of the amino acids flanking the transmembrane part, a different amount of bilayer ordering has been observed (*61*). Previous investigations of peptides in DMPC bilayers have, on the other hand, shown that a small decrease in bilayer order results from peptide interactions with or near the bilayer interface (*62*). Thus it seems as if the bPrPp adopts an orientation that increases the order of the bilayer, and the absence of amide exchange should therefore mainly be due to a rigid helical structure, which inserts in a

transmembrane orientation. This is different to what is seen for the well-studied cell-penetrating peptide penetratin, which is seen to reside close to or within the interface or headgroup region of the membrane (*63*−*65*).

To our surprise we did not see any signals in the NMR spectrum of the peptide in $q = 0.5$ bicelles, despite the fact that the CD data showed a similar induced structure in bicelles as in DHPC micelles (Figure 1). There could be several reasons for this. If the peptide undergoes conformational exchange, exchange broadening of the peaks could occur, leading to vanishing signals. It is, however, unlikely that all signals are exchange broadened beyond detection. No corresponding exchange phenomenon could be observed for the peptide in DHPC.

The peptide may induce bicelle aggregation to produce a bicelle−peptide complex that is simply too large, making the signals in the spectrum too broad to be observed. Finally, the internal motion of the peptide and/or lipids could somehow be reduced, again making the signals too broad. The results of the diffusion measurements show that the bicelles on average become larger when bPrPp is bound (Table 2). The long axis of the pure bicelle is estimated to ∼105 Å and the short axis to ∼24 Å. When bPrPp is added, the long axis becomes ∼117 Å and the short axis ∼27 Å. The increase in size is not large enough to indicate that peptide-induced bicelle aggregation occurs. Peptide aggregation in the bicelle, however, cannot be excluded. Care should, however, be taken in drawing conclusions about size estimates for peptide−lipid aggregates from translational diffusion data, since these estimates have been shown to differ from results obtained by other means, possible due to the dependence of the hydration layer (*66*). Nevertheless, the increase in size does not seem large enough to indicate the formation of large phospholipid aggregates in the present case. The diffusion coefficients are in fact similar in magnitude to what has previously been observed for peptide−bicelle complexes, in which reasonable NMR spectra could readily be observed (*55*, *67*).

The ^{2}H quadrupolar splittings of the DMPC acyl chain deuterons revealed that the peptide has the effect of increasing the order of positions 5−7 in the acyl chains, which, on the other hand, could very well explain the lack of NMR signals in small isotropic bicelles. If the peptide adopts a conformation, and a position, that renders the acyl chains more immobile, broadening of signals should occur. The fact that we see no amide exchange within the helical part of the peptide supports the second hypothesis, that the peptide adopts a rigid structure in which lack of internal motions leads to broadening of the resonances beyond detection. This is somewhat different from what is known about the structure and orientation of cell-penetrating peptides in general, in that they normally reside close to the membrane surface and seem to display high internal mobility within the membrane mimetic. The sequence of the bPrPp differs from the typical amphipathic properties seen in, e.g., penetratin and instead contains a stretch of hydrophobic residues (Ile10−Met17). This is likely to affect the properties of the bPrPp peptide as a CPP and make it less benign than, e.g., penetratin in its membrane interactions. This property could possibly be related to toxicity coupled to membrane translocation in the biological effects of bPrP and its potential cargo comprised of the remainder of the PrP.

ACKNOWLEDGMENT

We thank Dick Sandström for valuable discussions.

REFERENCES

1. Prusiner, S. B. (1997) Prion diseases and the BSE crisis, *Science 278*, 245−251.
2. Prusiner, S. B. (1982) Novel proteinaceous infectious particles cause scrapie, *Science 24*, 136−144.
3. Oesch, B., Westaway, D., Walchli, M., McKinley, M. P., Kent, S. B., Aebersold, R., Barry, R. A., Tempst, P., Teplow, D. B., Hood, L. E., Prusiner, S. B., and Weismann, C. (1985) A cellular gene encodes scrapie PrP 27−30 protein, *Cell 40*, 735−746.
4. McKinley, M. P., Taraboulos, A., Kenaga, L., Serban, D., Stieber, A., Dearmond, S. J., Prusiner, S. B., and Gonatas, N. (1991) Ultrastructural-localization of scrapie prion proteins in cytoplasmic vesicles of infected cultured-cells, *Lab. Invest. 65*, 622−630.
5. Prusiner, S. B. (1998) Prions, *Proc. Natl. Acad. Sci. U.S.A. 95*, 13363−13383.
6. Caughey, B., and Chesebro, B. (1997) Prion protein and the transmissible spongiform encephalopathies, *Trends Cell Biol. 7*, 56−62.
7. Prusiner, S. B. (1991) Molecular-biology of prion diseases, *Science 252*, 1515−1522.
8. Kocisko, D. A., Come, J. H., Priola, S. A., Chesebro, B., Raymond, G. J., Lansbury, P. T., and Caughey, B. (1994) Cell-free formation of protease-resistant prion protein, *Nature 370*, 471−474.
9. Harris, D. A. (2003) Trafficking, turnover and membrane topology of PrP, *Br. Med. Bull. 66*, 71−85.
10. Sunyach, C., Jen, A., Deng, J., Fitzgerald, K. T., Frobert, Y., Grassi, J., McCaffrey, M. W., and Morris, R. (2003) The mechanism of internalization of glycosylphosphatidylinositol-anchored prion protein, *EMBO J. 22*, 3591−3601.
11. Kazlauskaite, J., Sanghera, N., Sylvester, I., Venien-Bryan, C., and Pinheiro, T. J. T. (2003) Structural changes of the prion protein in lipid membranes leading to aggregation and fibrillization, *Biochemistry 42*, 3295−3304.
12. Sanghera, N., and Pinheiro, T. J. T. (2002) Binding of prion protein to lipid membranes and implications for prion conversion, *J. Mol. Biol. 315*, 1241−1256.
13. Stahl, N., Borchelt, D. R., Hsiao, K., and Prusiner, S. B. (1987) Scrapie prion protein contains a phosphatidylinositol glycolipid, *Cell 51*, 229−240.
14. Vey, M., Pilkuhn, S., Wille, H., Nixon, R., DeArmond, S. J., Smart, E. J., Anderson, R. W. G., Taraboulos, A., and Prusiner, S. B. (1996) Subcellular colocalization of the cellular and scrapie prion proteins in caveolae-like membranous domains, *Proc. Natl. Acad. Sci. U.S.A. 93*, 14945−14949.
15. Navslavsky, N., Stein, R., Yanai, A., Friedlander, G., and Taraboulos, A. (1997) Characterization of detergent-insoluble complexes containing the cellular prion protein and its scrapie isoform, *J. Biol. Chem. 272*, 6324−6331.
16. Leclerc, E., Peretz, D., Ball, H., Solforosi, L., Legname, G., Safar, J., Serban, A., Prusiner, S. B., Burton, D. R., and Williamson, R. A. (2003) Conformation of PrP^C on the cell surface as probed by antibodies, *J. Mol. Biol. 326*, 475−483.
17. Renner, C., Fiori, S., Fiorino, F., Landgraf, D., Deluca, D., Mentler, M., Grantner, K., Parak, F. G., Kretzschmar, H., and Moroder, L. (2003) Micellar environments induce structuring of the N-terminal tail of the prion protein, *Biopolymers 73*, 421−433.
18. Eberl, H., Tittmann, P., and Glockshuber, R. (2004) Characterization of recombinant membrane-attached full-length prion protein, *J. Biol. Chem. 279*, 25058−25065.
19. Garcia, F. L., Zahn, R., Riek, R., and Wüthrich, K. (2000) NMR structure of the bovine prion protein, *Proc. Natl. Acad. Sci. U.S.A. 97*, 8334−8339.
20. Nunziante, M., Gilch, S., and Schatzl, H. M. (2003) Essential role of the prion protein N terminus in subcellular trafficking and half-life of cellular prion protein, *J. Biol. Chem. 278*, 3726−3734.
21. Walmsley, A. R., Zeng, F., and Hooper, N. M. (2003) The N-terminal region of the prion protein ectodomain contains a lipid raft targeting determinant, *J. Biol. Chem. 278*, 37241−37248.
22. Langel, Ü., Ed. (2002) *Cell Penetrating Peptides. Processes And Applications*, CRC Press, Boca Raton, London, New York, and Washington, DC.

23. Lundberg, P., Magzoub, M., Lindberg, M., Hällbrink, M., Jarvet, J., Eriksson, L. E. G., Langel, Ü., and Gräslund, A. (2002) Cell membrane translocation of the N-terminal (1−28) part of the prion protein, *Biochem. Biophys. Res. Commun. 299*, 85−90.
24. Stewart, R. S., and Harris, D. A. (2001) Most pathogenic mutations do not alter the membrane topology of the prion protein, *J. Biol. Chem. 276*, 2212−2220.
25. Hegde, R. S., Tremblay, P., Groth, D., DeArmond, S. J., Prusiner, S. B., and Lingappa, V. R. (1999) Transmissible and genetic prion diseases share a common pathway of neurodegeneration, *Nature 402*, 822−826.
26. Hegde, R. S., Mastrianni, J. A., Scott, M. R., DeFea, K. A., Tremblay, P., Torchia, M., DeArmond, S. J., Prusiner, S. B., and Lingappa, V. R. (1998) A transmembrane form of the prion protein in neurodegenerative disease, *Science 279*, 827−834.
27. Ott, C. M., and Lingappa, V. R. (2004) Signal sequences influence membrane integration of the prion protein, *Biochemistry 43*, 11973−11982.
28. Stewart, R. S., Drisaldi, B., and Harris, D. A. (2001) A transmembrane form of the prion protein contains an uncleaved signal peptide and is retained in the endoplasmic reticululm, *Mol. Biol. Cell 12*, 881−889.
29. Stewart, R. S., and Harris, D. A. (2003) Mutational analysis of topological determinants in prion protein (PrP) and measurement of transmembrane and cytosolic PrP during prion infection, *J. Biol. Chem. 278*, 45960−45968.
30. Ma, J., Wollmann, R., and Lindquist, S. (2002) Neurotoxicity and neurodegeneration when PrP accumulates in the cytosol, *Science 298*, 1781−1785.
31. Ma, J., and Lindquist, S. (2002) Conversion of PrP to a self-perpetuating PrP^{SC}-like conformation in the cytosol, *Science 298*, 1785−1788.
32. Terrone, D., Sang, S. L. W., Roudaia, L., and Silvius, J. R. (2003) Penetratin and related cell-penetrating cationic peptides can translocate across lipid bilayers in the presence of a transbilayer potential, *Biochemistry 42*, 13787−13799.
33. Greenfield, N., and Fasman, G. D. (1969) Computed circular dichroism spectra for the evaluation of protein conformation, *Biochemistry 8*, 4108−4116.
34. Braunschweiler, L., and Ernst, R. R. (1983) Coherence transfer by isotropic mixing: application to proton correlation spectroscopy, *J. Magn. Reson. 53*, 521−528.
35. Jeener, J., Meier, B., Bachman, P., and Ernst, R. R. (1979) Investigation of exchange process by two-dimensional NMR spectroscopy, *J. Chem. Phys. 71*, 4546−4563.
36. Piotto, M., Saudek, V., and Sklenár, V. (1992) Gradient-tailored excitation for single-quantum nmr-spectroscopy of aqueous-solutions, *J. Biomol. NMR 2*, 661−665.
37. Stejskal, E. O., and Tanner, J. E. (1965) Spin diffusion measurements: spin-echoes in the presence of a time-dependent field gradient, *J. Chem. Phys. 42*, 288−292.
38. Callaghan, P. T., Komlosh, M. E., and Nyden, M. (1998) High magnetic field gradient PGSE NMR in the presence of a large polarizing field, *J. Magn. Reson. 133*, 177−182.
39. Vonmeerwall, E., and Kamat, M. (1989) Effect of residual field gradients on pulsed-gradient NMR diffusion measurements, *J. Magn. Reson. 83*, 309−323.
40. Damberg, P., Jarvet, J., and Gräslund, A. (2001) Accurate measurement of translational diffusion coefficients: A practical method to account for nonlinear gradients, *J. Magn. Reson. 148*, 343−348.
41. Cantor C. R., and Shimmel P. R. (1980) *Biophysical chemistry, Part II, Techniques for the study of biological structure and function*, W. H. Freeman, San Francisco.
42. Glover, K. J., Whiles, J. A., Wu, G., Yu, N., Deems, R., Struppe, J. O., Stark, R. E., Komives, E. A., and Vold, R. R. (2001) Structural evaluation of phospholipid bicelles for solution-state studies of membrane-associated biomolecules, *Biophys. J. 81*, 2163−2171.
43. Vold, R. R., and Prosser, R. S. (1996) Magnetically oriented phospholipid bilayered micelles for structural studies of polypeptides. Does the ideal bicelle exist?, *J. Magn. Reson. 113*, 267−271.
44. Davis, J. H., Jeffery, K. R., Bloom, M., Valic, M. I., and Higgs, T. P. (1976) Quadrupolar echo deuterium magnetic resonance spectroscopy in ordered hydrocarbon chains, *Chem. Phys. Lett. 42*, 390−394.
45. Seelig, J. (1977) Deuterium magnetic resonace: theory and application to lipid membranes, *Q. Rev. Biophys. 10*, 353−418.
46. Andersson, A., and Mäler, L. (2002) NMR solution structure and dynamics of motilin in isotropic phospholipid bicellar solution, *J. Biomol. NMR 24*, 103−112.
47. Güntert, P., Mumenthaler, C., and Wüthrich, K. (1997) Torsion angle dynamics for NMR structure calculation with the new program DYANA, *J. Mol. Biol. 273*, 283−298.
48. Laskowski, R. A., Macarthur, M. W., Moss, D. S., and Thornton, J. M. (1993) Procheck − a program to check the stereochemical quality of protein structures, *J. Appl. Crystallogr. 26*, 283−291.
49. Magzoub, M., Oglecka, K., Lundberg, P., Langel, Ü., Eriksson, L. E. G., and Gräslund, A. (2004) unpublished results.
50. Wishart, D. S., and Sykes, B. D. (1994) Chemical-shifts as a tool for structure determination, *Methods Enzymol. 239*, 363−392.
51. Urbina, J. A., Pekerar, S., Le, H. B., Patterson, J., Montez, B., and Oldfield, E. (1995) Molecular order and dynamics of phosphatidylcholine bilayer-membranes in the presence of cholesterol, ergosterol and lanosterol: a comparative-study using ^{2}H-, ^{13}C-, and ^{31}P-NMR spectroscopy, *Biochim. Biophys. Acta 1238*, 163−176.
52. de Planque, M. R. R., Greathouse, D. V., Koeppe, R. E., Schafer, H., Marsh, D., and Killian, J. A. (1998) Influence of lipid/peptide hydrophobic mismatch on the thickness of diacylphosphatidylcholine bilayers. A ^{2}H NMR and ESR study using designed transmembrane alpha-helical peptides and gramicidin A, *Biochemistry 37*, 9333−9345.
53. Killian, J. A. (2003) Synthetic peptides as models for intrinsic membrane proteins, *FEBS Lett. 555*, 134−138.
54. Killian, J. A. (1998) Hydrophobic mismatch between proteins and lipids in membranes, *Biochim. Biophys. Acta 1376*, 401−416.
55. Andersson, A., and Mäler, L. (2003) Motilin-bicelle interactions: membrane position and translational diffusion, *FEBS Lett. 545*, 139−143.
56. Glover, K. J., Whiles, J. A., Wu, G. H., Yu, N. J., Deems, R., Struppe, J. O., Stark, R. E., Komives, E. A., and Vold, R. R. (2001) Structural evaluation of phospholipid bicelles for solution-state studies of membrane-associated biomolecules, *Biophys. J. 81*, 2163−2171.
57. Kim, S. J., Rahbar, R., and Hegde, R. S. (2001) Combinatorial control of prion protein biogenesis by the signal sequence and transmembrane domain, *J. Biol. Chem. 276*, 26132−26140.
58. Bai, Y. W., Milne, J. S., Mayne, L., and Englander, S. W. (1993) Primary structure effects on peptide group hydrogen-exchange, *Proteins 17*, 75−86.
59. Connelly, G. P., Bai, Y. W., Jeng, M. F., and Englander, S. W. (1993) Isotope effects in peptide group hydrogen-exchange, *Proteins 17*, 87−92.
60. Sperotto, M. M., and Mouritsen, O. G. (1988) Dependence of lipid-membrane phase-transition temperature on the mismatch of protein and lipid hydrophobic thickness, *Eur. Biophys. J. 16*, 1−10.
61. de Planque, M. R. R., Boots, J. W. P., Rijkers, D. T. S., Liskamp, R. M. J., Greathouse, D. V., and Killian, J. A. (2002) The effects of hydrophobic mismatch between phosphatidylcholine bilayers and transmembrane alpha-helical peptides depend on the nature of interfacially exposed aromatic and charged residues, *Biochemistry 41*, 8396−8404.
62. Banerjee, U., Zidovetzki, R., Birge, R. R., and Chan, S. I. (1985) Interaction of alamethicin with lecithin bilayers−a P^{31} and H^{2} NMR-study, *Biochemistry 24*, 7621−7627.
63. Drin, G., Mazel, M., Clair, P., Mathieu, D., Kaczorek, M., and Temsamani, J. (2001) Physicochemical requirements for cellular uptake of pAntp peptide−Role of lipid-binding affinity, *Eur. J. Biochem. 268*, 1304−1314.
64. Drin, G., Demene, H., Temsamani, J., and Brasseur, R. (2001) Translocation of the pAntp peptide and its amphipathic analogue AP-2AL, *Biochemistry 40*, 1824−1834.
65. Magzoub, M., Eriksson, L. E. G., and Gräslund, A. (2003) Comparison of the interaction, positioning, structure induction and membrane perturbation of cell-penetrating peptides and nontranslocating variants with phospholipid vesicles, *Biophys. Chem. 103*, 271−288.
66. Chou, J. J., Baber, J. L., and Bax, A. (2004) Characterization of phospholipid mixed micelles by translational diffusion, *J. Biomol. NMR 29*, 299−308.
67. Andersson, A., Almqvist, J., Hagn, F., and Mäler, L. (2004) Diffusion and dynamics of penetratin in different membrane mimicking media, *Biochim. Biophys. Acta 1661*, 18−25.

BI0485070